Wavefront Sensing and Control for a Next Generation Space Telescope

David Redding, Scott Basinger, Andrew E. Lowman, Andy Kissil
Jet Propulsion Laboratory, California Institute of Technology

Pierre Bely
Space Telescope Science Institute

Richard Burg
Johns Hopkins University

Rick Lyon
University of Maryland

Gary Mosier, Mike Femiano and Mark Wilson
Goddard Space Flight Center, National Aeronautics and Space Administration

David Jacobson and John Rakoczy
Marshall Space Flight Center, National Aeronautics and Space Administration

James Hadaway
University of Alabama

ABSTRACT

The Next Generation Space Telescope will provide more than ten times the collecting area of the Hubble Space Telescope in a package that fits into the shroud of an expendable launch vehicle. Active optical controls will compensate the optical effects of deployment and fabrication errors, thermal deformations, guiding errors, and vibrations from spacecraft hardware. Building in a high degree of on-orbit adjustability dramatically reduces requirements on structural stability and mass, allowing NGST to break the traditional telescope cost paradigm.

This paper illustrates the operation and performance expected for initial telescope alignment, segment phasing, and fine figure control for the NGST "Yardstick" design. The Yardstick is a deployed, 8-meter aperture telescope, passively cooled to cryogenic temperatures. It is equipped with actuators on its main optics and a deformable quartenary mirror. Guiding is split between a fast steering mirror and the spacecraft attitude control system. Sensing is provided by infra-red science cameras - no dedicated wavefront or guiding sensor is used.

Wavefront control occurs in periodic dedicated sessions, while observing bright, unresolved natural objects. The figure is held passively during observations.

Initial telescope alignment uses focus/coma sweeps to align and phase to within a few tens of waves. Coarse segment phasing uses dispersed-fringe sensing and image sharpening to phase to about 1 wave. Fine figure control using phase retrieval wavefront sensing drives the segments and deformable mirror to achieve diffraction-limited final performance.

This process is illustrated using detailed simulation models to show imagery and performance at every phase of the wavefront control operation. Statistical results illustrate performance over a range of conditions. Alternative approaches are investigated, to motivate trades in actuator density, sensor type, fabrication and deployment tolerances, optical design, and other parameters.

1.INTRODUCTION

The Next Generation Space Telescope (NGST) will be a large-aperture, extremely light weight, cryogenic, infra-red space telescope, providing imagery and spectrometry from 1 um to 16 um wavelength.[1-2] It will be diffraction limited at a wavelength of 2 um. With an aperture of about 8 m, NGST will provide about

ten times the collecting area of the Hubble Space Telescope, in a package that weighs only 3500 kg and fits into the shroud of a small expendable launch vehicle.

The NGST will be subject to disturbances from a variety of sources. Those that impact imaging performance include optical manufacturing errors, thermal deformations, shifts in alignments during launch, deployment errors, and spacecraft-induced vibrations. To compensate these effects, and to perform initial alignment of the telescope following launch, NGST will be equipped with a wavefront sensing and control system.

This paper examines the architecture and performance of the optical control system for the NGST "Yardstick" design. The Yardstick is a point design developed by a team led by the Goddard Space Flight Center. It is intended to provide context and focus for the NASA team, to help in evaluating feasibility and performance of NGST, to identify new technology requirements, to resolve technological issues, and to prepare the government team for the procurement of the NGST spacecraft. Several other designs are also under active study by industry, NASA and ESA teams.[1]

Most of the designs being considered, including the Yardstick, use deployed, segmented primary mirror optics and a deployed secondary mirror. A large sunshield shades the spacecraft, allowing it to cool passively to cryogenic temperatures (Fig. 1). Orbiting far from earth, around the Earth-Sun L2 point for the Yardstick, thermal and dynamical environment is benign, providing for a high degree of passive stability once the spacecraft has cooled to operational temperatures.

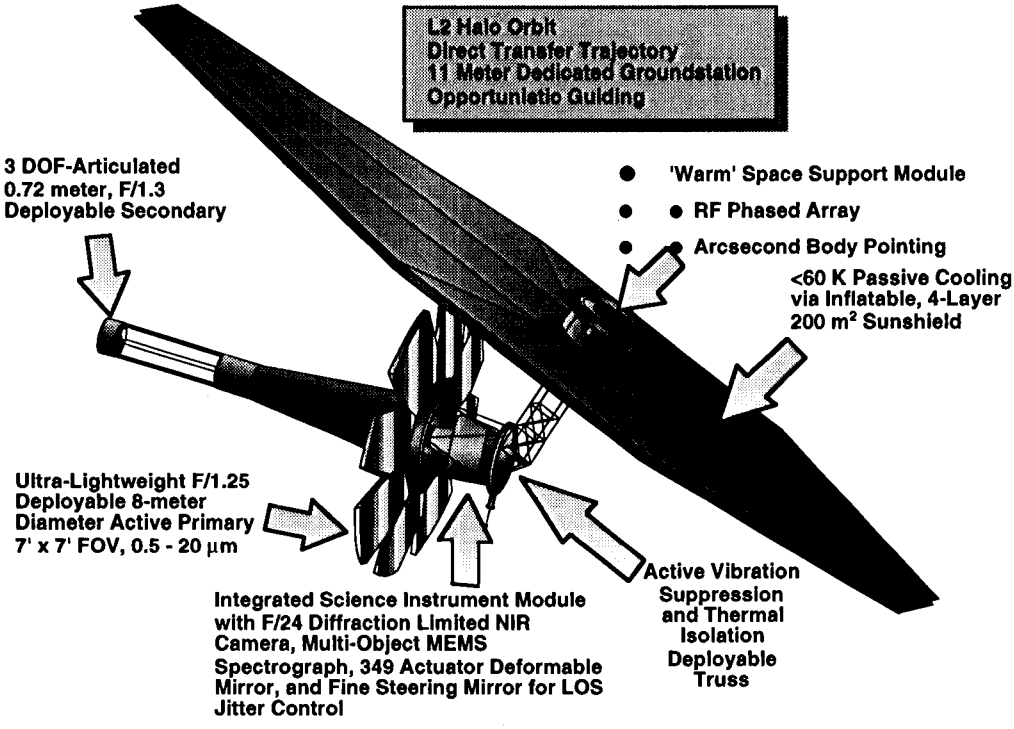

Figure 1. The NGST Yardstick configuration.

The post-launch, post-deployment condition of the NGST optics should be expected to be poor. Segment figure will have changed significantly during cooling from ambient to orbital temperatures. If this is not predicted and compensated precisely, residual wavefront error of a few waves will be induced. Segments and the SM may be misaligned by millimeters and milliradians. Initially, there may be no light on the focal plane.

The first task for the NGST wavefront control system is thus to acquire and align the secondary and primary segments to the science instruments. This includes initial coarse phasing of the primary mirror

segments. In the Yardstick design, this is accomplished by a "coarse figure initialization" controller. This control utilizes the Near IR science imaging camera, during dedicated observations of a bright unresolved star. For its wavefront sensing task the NIR camera is augmented by a grism to form a dispersed-fringe phase sensor, and a defocus mechanism. Both imagery and dispersed fringe data are used to determine the control. The primary mirror segments and the secondary mirror are actuated in 5 or 6 degrees of freedom. The coarse alignment process will be iterative and require some time. Coarse initialization is expected to be needed only once, at the beginning of the mission.

Following coarse initialization, the primary mirror is expected to be aligned and phased to within the figure quality of the segments, perhaps as much as a few waves at the target 2 um wavelength. Improving optical quality to within the diffraction limit at that wavelength is the task of the "fine figure initialization controller." This mode uses focus-diverse phase retrieval to measure the overall wavefront. The wavefront estimate is then processed to determine segment and deformable-mirror (DM) commands to drive the wavefront towards zero. These are implemented and the process is iterated until the performance objective is met.

Both control stages are described in some detail later in this paper. Guiding is split between a fast steering mirror and the spacecraft attitude control system. Sensing for the fine guiding, as for the WF control, is provided by the IR science cameras - no dedicated wavefront or guiding sensor is used. A small portion of one of the Near IR camera detectors is dedicated to the guiding function, read out at a high rate and used to stabilize the line of sight.[5]

Wavefront control occurs in periodic dedicated sessions, while observing bright, unresolved natural objects. The figure is held passively during observations.

The NGST optical control system is the last line of defence against a wide range of disturbing effects, ranging from optical manufacturing errors to thermal deformations, from deployment errors to control errors, and performed in the presence of spacecraft-induced vibrations. The wavefront control system takes the place of the massive, stiff structure usually utilized to preserve alignments and optical quality. By providing a high degree of on-orbit adjustability, the WF control system dramatically reduces requirements on structural and thermal stability and mass, allowing NGST to break the traditional telescope cost paradigm.

The performance of the optical controls is a direct function of disturbing factors from every subsystem of the spacecraft. This discussion, therefore, deals with the NGST OTA, SSM and SIM as an integrated system, using as its standard of performance the bottom-line scientific performance of the telescope as a whole. Evaluation of control performance, and so of the end-to-end performance of the NGST Yardstick, is done in a computer modeling environment that combines finite-element structures models with ray-trace and diffraction-based optics, radiative heat-transfer and conduction models, as well as a full spaccraft attitude control system.[5]

Operation at a very high orbit such as L2 halo orbit Active optical controls will compensate the optical effects of deployment and fabrication errors, thermal deformations, guiding errors, and vibrations from spacecraft hardware.

This paper illustrates the operation and performance expected for initial telescope alignment, segment phasing, and fine figure control for the NGST "Yardstick" design. The Yardstick is a deployed, 8-meter aperture telescope, passively cooled to cryogenic temperatures. It is equipped with actuators on its main optics and a deformable quartenary mirror. Guiding is split between a fast steering mirror and the spacecraft attitude control system. Sensing is provided by infra-red science cameras - no dedicated wavefront or guiding sensor is used.

Wavefront control occurs in periodic dedicated sessions, while observing bright, unresolved natural objects. The figure is held passively during observations.

Initial telescope alignment uses focus/coma sweeps to align and phase to within a few tens of waves. Coarse segment phasing uses dispersed-fringe sensing and image sharpening to phase to about 1 wave. Fine figure control using phase retrieval wavefront sensing drives the segments and deformable mirror to achieve diffraction-limited final performance.

This process is illustrated using detailed simulation models to show imagery and performance at every phase of the wavefront control operation. Statistical results illustrate performance over a range of conditions. Alternative approaches are investigated, to motivate trades in actuator density, sensor type, fabrication and deployment tolerances, optical design, and other parameters.

The NGST optical control system will The optical control system is the last line of defence against a wide range of disturbing effects, ranging from optical manufacturing errors to thermal deformations, from deployment errors to spacecraft-induced vibrations. The performance of the optical controls is a direct function of disturbing factors from every subsystem of the spacecraft. This discussion, therefore, deals with the NGST OTA, SSM and SIM as an integrated system, using as its standard of performance the bottom-line scientific performance of the telescope as a whole.

This performance has been quantified using detailed integrated controls/structures/optics/thermal models of the various subsystems. This modeling activity has also integrated numerous people from across NASA and other organizations. In particular, Bob Beaman, Larry Craig, Greg Schunk of MSFC; Andy Kissil and Ali Behboud of JPL; and Greg Mosier and Cherie Congedo of GSFC contributed major portions of the integrated model. Dave Redding of JPL authored this presentation.

The Next Generation Space Telescope will be a complex system, with ambitious requirements in every subsystem contributing directly to the overall scientific performance of the mission. It will depend on several critical new technologies, like adaptive optics, extremely lightweight optics, cryogenic optics, etc.

The results presented here were computed using an integrated computational model of the NGST, as indicated here. This gives us the ability to accurately assess the scientific impact of design decisions made in each subsystem, and to trade off design parameters in one subsystem against parameters in other subsystems. It also gives us a software testbed -- a virtual NGST -- with which we can try different control algorithms and architectures.

The computer tools we used include NASTRAN, TRASYS, SINDA, IMOS, MACOS, VSIM and MATLAB.

2.SYSTEM DESCRIPTION

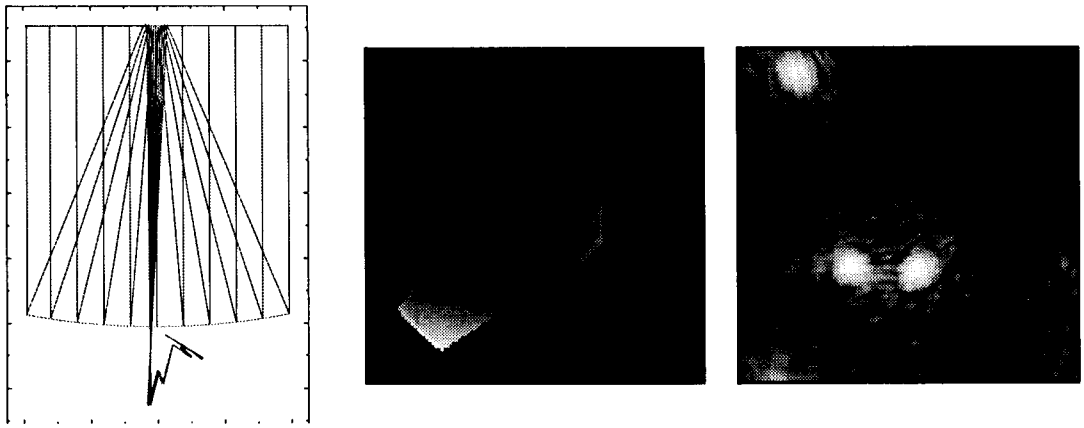

Figure 2. NGST Yardstick layout, pupil map, and aberrated image.

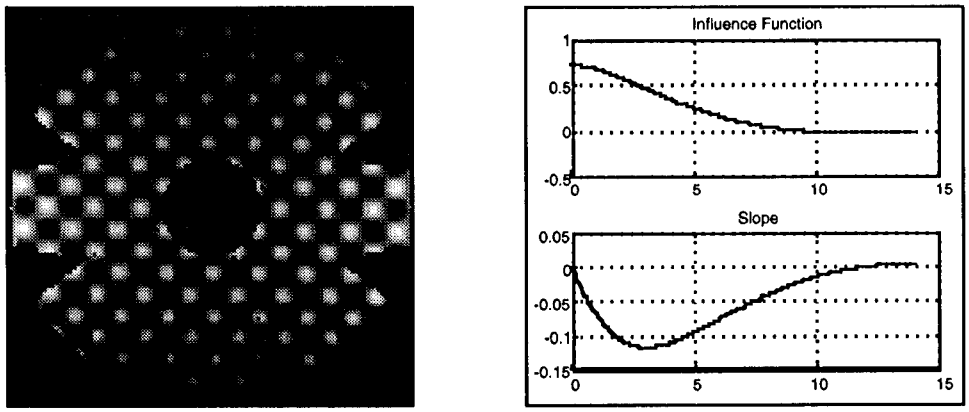

Figure 3. Deformable mirror.

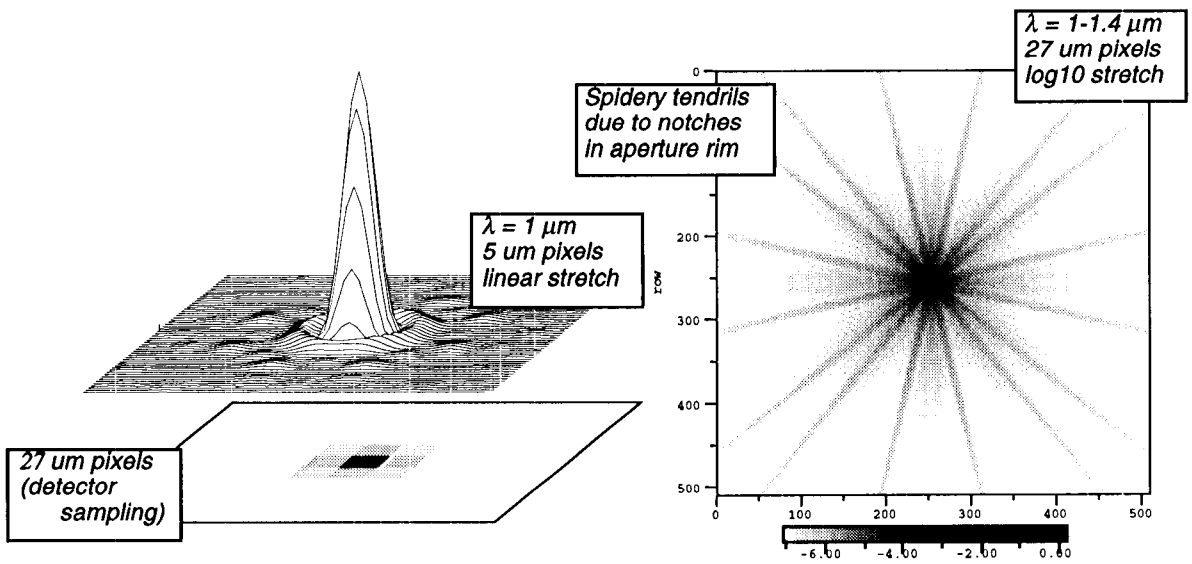

Figure 4. Nominal point-spread function.

3.WAVEFRONT SENSING AND CONTROL

The baseline NGST optical controller has just 2 modes: Coarse Initialization Control, wherein the initial alignment and phasing of the telescope is performed; and Fine Initialization Control, wherein the 9 primary mirror (PM) segments and the secondary mirror (SM) are phased, and the deformable quartenary mirror (DM) is set so as to minimize wavefront error (WFE) and maximize Strehl ratio (SR) for the ensuing observations. Initialization occurs while the telescope is observing a bright calibration star. It uses the Near-IR science camera for sensing.

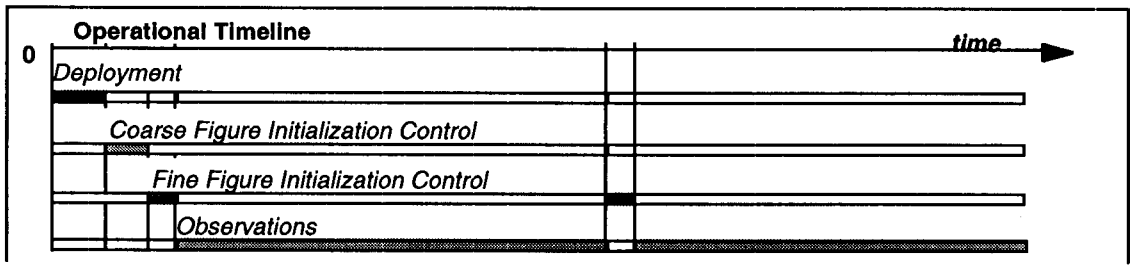

The current plan is to rely on passive structural stability to preserve alignments and phasing during observations. It remains to be seen whether this is really possible, given available materials and the thermal environment, as discussed later in this document.

A Figure Maintenance control system was also defined, and will be used if passive structural stability is not adequate. The Figure Maintenance controller utilizes a seperate laser metrology system to observe motions of the segments, SM and SIM with respect to each other, driving segment and SM actuators to preserve good optical quality, as discussed later.

The Coarse Initialization Controller is invoked upon first light following deployment on orbit. While observing a bright star, it utilizes a simple and robust Co-Alignment/Co-Phasing algorithm to first acquire the images produced by individual segments on the Near-IR camera focal plane, and then to co-align them 2 at a time. When 2 spots overlie, they can be co-phased. When phase differences are large, a spectral signal obtained using a GRISM in the Near-IR camera filter wheel is used to determine the absolute phase difference. These phase differences are removed by the segment actuators. When phase differences are within 1/2 wave, the GRISM is removed, and direct image sharpening is used to peak up the coherent image, which provides a very sensitive indicator of phase errors. When 2 segments have been cophased, one is moved out of the field, and another is brought in, and the process repeats until all are aligned and phased.

This procedure is capable of aligning pairs of segments to well within a wave. Alignments are somewhat compromised by having to work pairwise, which necessitates relying on actuatr accuracy and repeatibility to a high degree. An independent metrology might be required if this proves to be a problem.

The Co-Alignment/Co-Phasing algorithm will be run in a semi-autonomous mode with little human intervention.

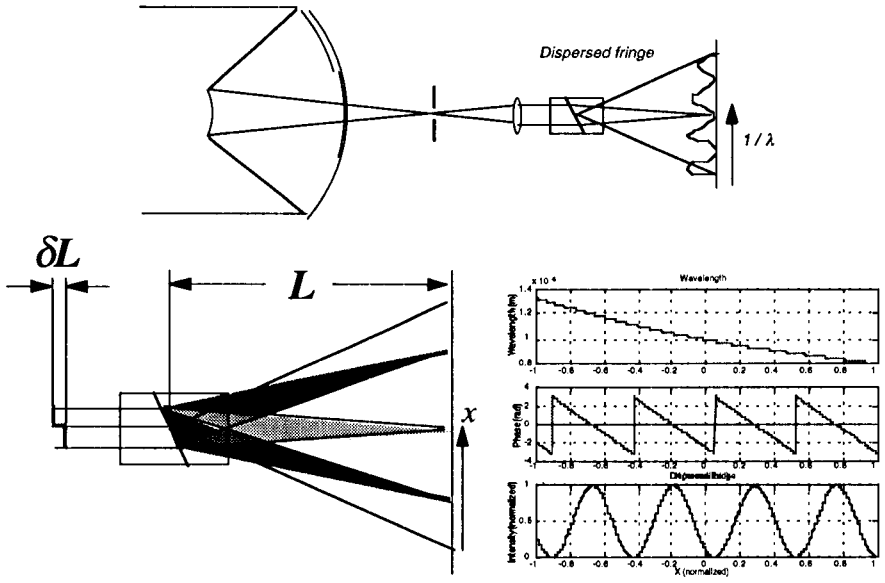

Figure 5. Dispersed-fringe sensor.

This illustrates the use of a GRISM in the filter wheel of the near-IR camera to spectrally spread the images of 2 segments out over the detector surface. These images are taken using a bright broad-band calibration star. Phase differences between the 2 segments cause the overlapping images to produce interference fringes. The period of these fringes is proportional to the absolute phase difference between the 2 segments.

Field at any x on detector sums contribution from 2 dephased segments:

$$E = E0 \exp(i\,(2p/l(x))\,L)\;(1 + \exp(i(2p/l(x)\,dL)$$

Phase difference dL is modulated by wavelength (which varies with x), causing dispersed spots to interfere

Fringe spacing along x is inversely proportional to dL

Sign is ambiguous

Use of this spread fringe phase sensor allows pairwise phasing to within 1/4 wave in just a few actuation steps. This phasing approach is in routine use at the Palomar Interferometer, where it is used to phase up widely-separated small apertures using starlight.

Fine Initialization Control picks up where the Coarse Initialization leaves off: with all segments, SM and SIM phased to within 1/4 wave or so (ultimately set by actuator accuracy). All segments are in place, and remain there throughout the Fine Initialization process.

The Fine Initialization controller utilizes defocussed calibration star images and computer processing using a "phase diversity" algorithm to estimate wavefront error. Focus is effected by a piston mirror within the SIM Near-IR camera. The required (massive) processing is actually performed on the ground, and the resulting segment and DM control commands are uplinked from the ground.

The expected accuracy, given good quality optics and actuators, will leave the telescope in a diffraction-limited condition (2 um wavelength).

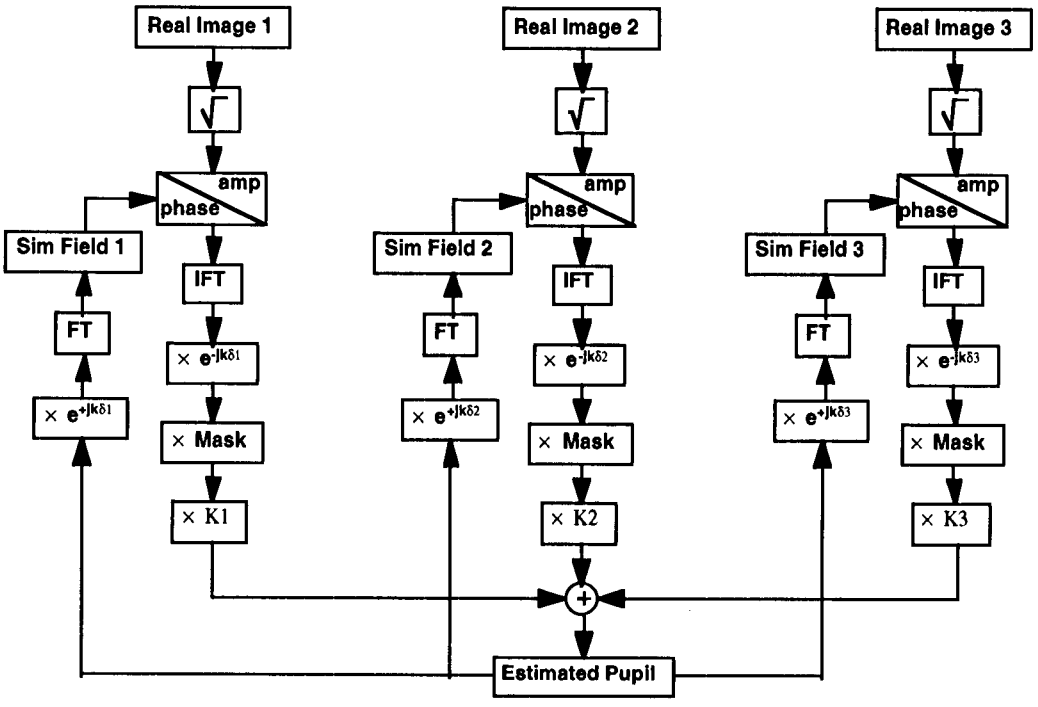

Figure 6. Focus-diverse iterative-transform phase retrieval algorithm.

Phase diversity refers to one of several candidate algorithms for computing phase from defocussed images: phase retrieval; prescription retrieval; curvature sensing; etc. As a baseline we assume that phase retrieval will be performed on 2 images, producing a roughly 2,000-point estimate of the wavefront. This is mapped to segment and DM commands using an optimal control algorithm. This sampling density is what is used in the results that follow.

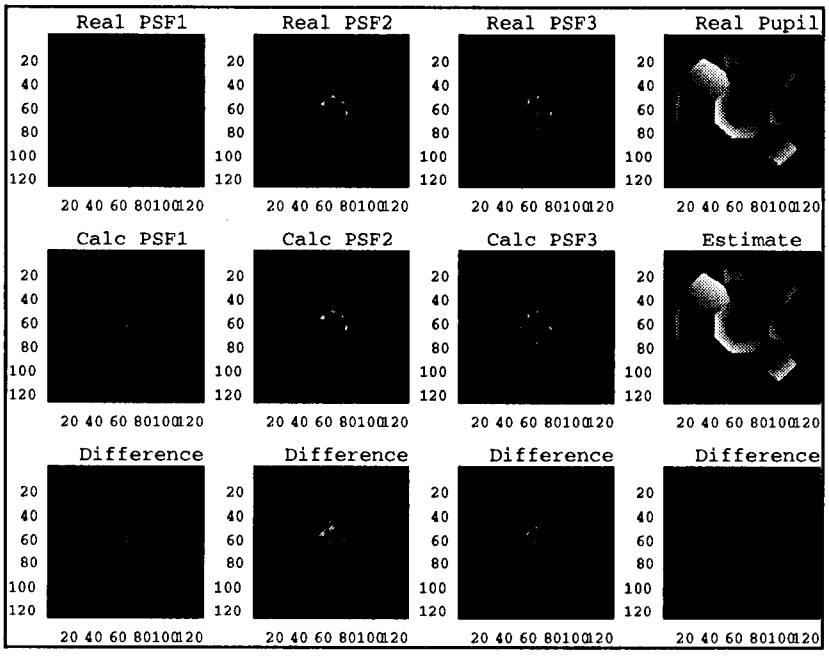

Figure 7. WF sensing example.

Phase diversity approaches were originally developed for electron microscopy. They have been applied effectively in optical testing and control, image restoration, and other applications by a number of practitioners.

There are several good alternative approaches for wavefront sensing, all of which require an additional sensor. Twyman-Green interferometers, shearing interferometers, Shack-Hartman sensors (together with a segment metrology system), all provide interesting options. We picked this approach as a baseline because it is the simplest, as it does not require additional sensors, and introduces a minimum of new error sources. The same basic algorithms can be run in any of the Near-IR (or even TIR) channels, at a wide range of wavelengths for improved dynamic range.

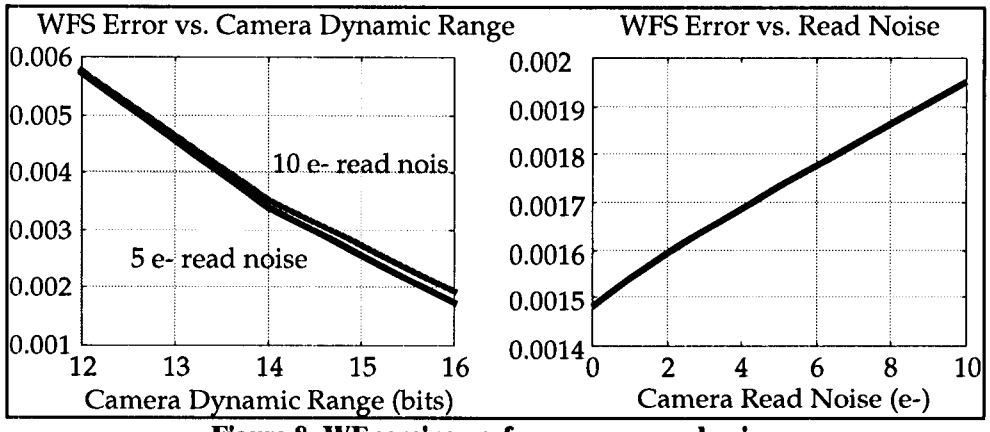

Figure 8. WF sensing performance vs. read noise.

WF control...

Matrix model of optical system

w: optical pathlength for each ray

x: element states: 6 rigid-body DOF per elt, plus Zernike deformation terms, plus 1044 FEM node displacements

u: control: 3 DOF per PM optic and 349 DM actuators

State transition equation

$w = C x + CA u$

Wavefront sensing generates estimate of w

Control law minimizes $J = 0.5\ wT\ w$

$u = -[ATCTCA]^{-1}\ ATCTwest + du = -Gwest + du$

Post-control residual error

$dw = W - CAG\ west + CA\ du$

Covariance analysis

$Wf = [I - CAGC]\ X\ [I - CAGC]\ T + CA\ U\ AT\ CT$

$std(WFE) = sqrt(trace(Wf))$

4.CONTROL EXAMPLE

5.FIGURE ERRORS

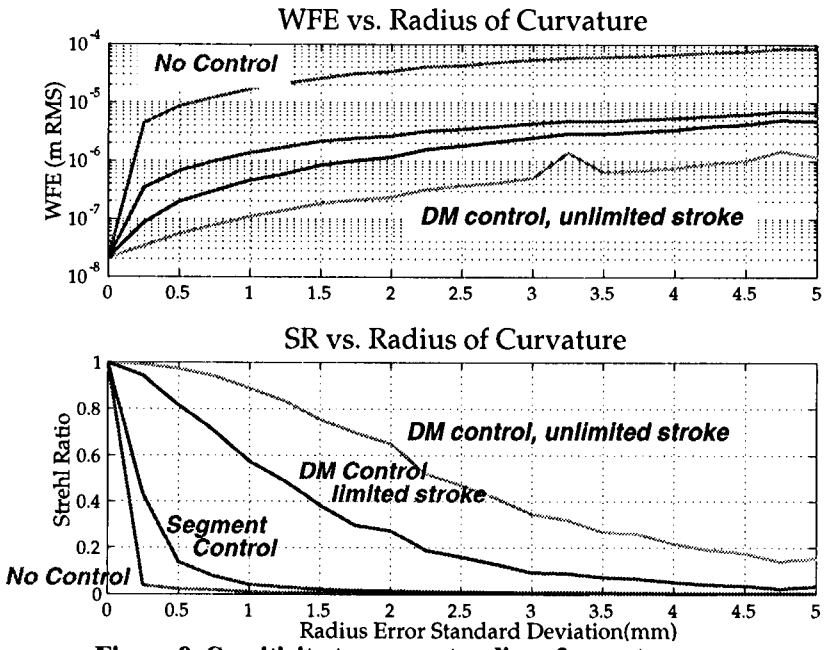

Figure 9. Sensitivity to segment radius of curvature.

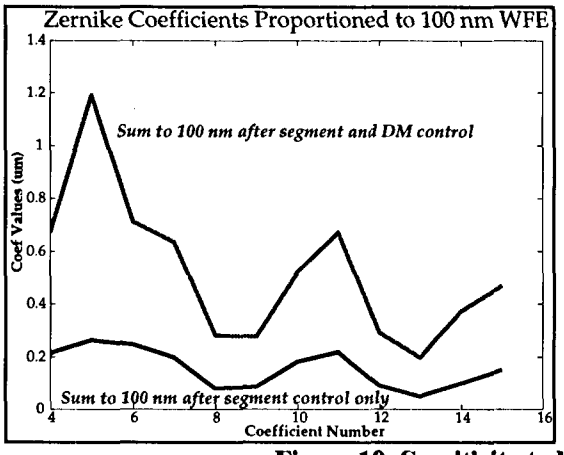

Low-Order Figure Error Budget

Total post-control WFE
100 nm

Term	Pre-control	Post-control
Z4	673 nm	43 nm
Z5	1191 nm	43 nm
Z6	711 nm	43 nm
Z7	637 nm	43 nm
Z8	283 nm	43 nm
Z9	278 nm	43 nm
Z10	520 nm	43 nm
Z11	673 nm	43 nm
Z12	292 nm	43 nm
Z13	199 nm	43 nm
Z14	373 nm	43 nm
Z15	469 nm	43 nm

Figure 10. Sensitivity to low-order figure errors.

6.ALIGNMENT ERRORS

The next 3 charts illustrate a single simulated control example. The ray-trace shows the basic layout of the optics; there are pre- and post- control wavefront error plots and the corresponding simulated images.

This example (and the other examples presented here) were computed using a 125x125 grid of rays traversing 21 optical elements, including all segments, the DM and FSM, and the detector; as driven variously by random deployment errors, random figure errors, thermally or dynamically driven structural deformations; and as controlled by the segment and DM actuators.

This example takes a random deployment error condition (computed as a Gaussian distribution over the 54 segment DOFs with uniform 100 um/urad variance). This chart shows the effect of the segment control only: the initial 612 um WFE is reduced by a factor of 3537 to a WFE of 173 nm. The resulting Strehl goes from zero to 0.5 of the on-axis peak intensity.

Note that the Strehl metric used here is the ratio of the peak intensity of a PSF to the ideal on-axis PSF (perfect optics, but with the NGST serrated aperture). The true Strehl is with respect to a annular aperture; this peaks out at 0.75 for the NGST.

The next step in the control process is to set the deformable mirror. This slide shows the DM at its pupil in the NGST SIM optical bench. Note the distortion of the pupil, which is fully accounted for in our integrated model. Note also the "smooth" response of these non-ideal actuators, which were commanded in a "waffle" mode.

The actuators are modeled using an influence function derived from first principles, with parameters set to match the response of ITEK mirror data. As shown, the response is fairly nonlinear, and extend over a fairly large area. This modeling approach does a relatively poor job of capturing the DC response of the real DM, as it is subject to "pinning." The model results are generally pessimistic as a consequence.

DM technology is well established, with several of these devices having accumulated many hundreds of hours running at several hundred Hertz as part of ground-based adaptive optics systems. The challenges for the NGST DM are to provide reliable performance at very low temperatures. Actuator properties and face-sheet quality and resilience are critical and unknown at this point. Further technology work is required in this area. An alternative to using the DM is to directly bend the PM segments, a more challenging mechanization job, but one with payoffs in control system dynamic range as well as potentially a more feasible actuator technology.

This chart continues our deployment-error example, showing the effect of controlling the DM. The upper WF plot and image are what was obtained previously by segment control. The bottom WF and image show residuals after the DM control is applied.

The final WFE is actually less than the nominal WFE, and the SRT is greater than the nominale SR, as the controller was set to flatten the WF. This has the undesirable effect of eliminating some of the field correction required to get a wide field-of-view in the Near-IR camera! We ran it this way simply to show the inherent performance of the controller. Normally we set the controller to drive the WF to the nominal WF.

We have tested the FOV of the Near-IR camera with the DM set to correct large aberrations, and have noticed a small drop in SR as we move off-axis. This is due in part to imperfect placement of the mirror (not all of the mirror is exactly at an image of the PM) and to the large pupil magnification of the DM. Alternative optical designs which increase pupil size are to be preferred, as they reduce pupil magnification and increase available DM stroke and actuator density.

Single-point simulations such as the preceeding provide good insight into the error and control processes. They are not, however, statistically significant. To compute response of the system over a wider range of paramenters we use Monte Carlo simulation and covariance analysis techniques. The latter especially provides a rapid way of generalizing integrated system performance over a wide range of conditions. Two examples follow...

This chart generalizes the results of the previous example over a very wide range of possible deployment errors. Here "deployment" error is any effect that translates or rotates any of the PM optics. The x-axis shows the deployment error variance: really the value of the (uniform) variance of each of the 6DOF error terms for each of the 9 segments. The y-axis shows the WFE for each of the various curves.

The upper curve shows the uncontrolled response of the system: WFE goes linearly with deployment error. The next curve down shows the effect of (3DOF) segment control only. It hits a noise floor set by the variance of the segment actuators. The lowest curve shows the effect of segment and DM control; it is about 10x lower than the segment control only curve.

The lowest noise floor is labeled "DM noise floor," but it is actually set by the segment actuator noise level. It has to do with the amount of segment edge discontinuity left in the pupil. These discontinuities are difficult for the DM to counter. The optimal controller knows this, and actually drives the segments to minimize edge discontinuities, letting the DM clean up the bulk figure errors. This noise floor can be lowered by using more DM actuators.

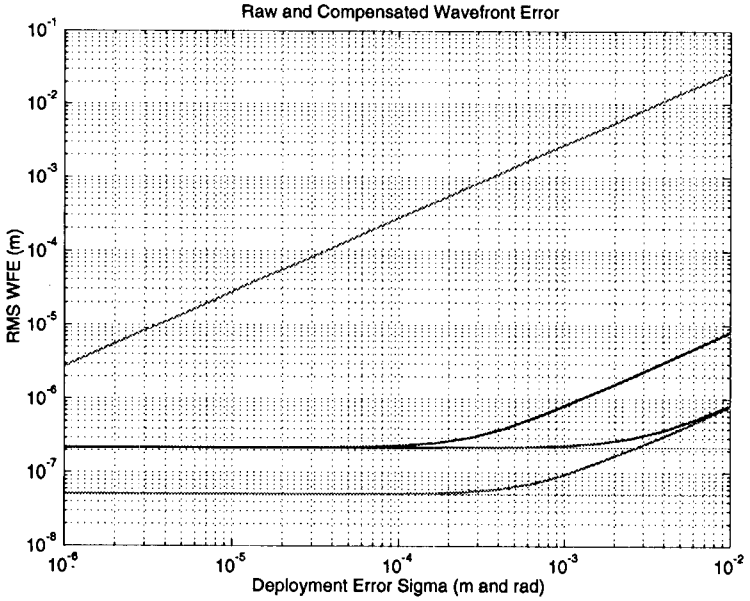

NGST 8-Petal configuration
8 meter aperture
F/1.25 primary
F/24 system
λ = 1.0 μm (0% bandpass)
Random initial segment state errors
Optimal WF controller
Set DM and segments together
Follow up with DM only
Phase sensing
Results via covariance analysis

Deployment error in 6DOF
Uniform variance
Segment actuation in 3DOF
Segment actuation error 8e-8 rad & m
DM actuation error 1e-9 m
Sensing error 1e-12 m

Figure 11. Alignment performance.

7.THERMAL DEFORMATIONS

Cryogenic operation presents a major challenge for NGST, and one of the main areas of concern is here in the thermal deformation of the optics as they go from the test enviroment to on-orbit conditions. The picture on the right indicates the temperatures expected in operation at L2.

Two cases are considered. The WF plot on the left shows the deformations expected at 30°K for a telescop that was figured at room temperature. As shown, there is substantial deformation of both the segments and the support structure (whic leads to rigid-body displacemens of the segments wrt each other). The WFE resulting is 62 um, smaller than the bulk displacements due to the uniform, spherical form of the deformations.

The second case is the one baselined for the NGST. It assumes optics that are figured at LN2 temperatures, which is well below the bulk of the deformation curve hump for this material (Be). The result is smaller deformation on orbit.

The effect of the optical control system on the cold-figured PM case from the preceding chart is shown here. The result is a SR of 96 % at 1 um wavelength.

The main concern from this example is the DM stroke required to compensate the wavefront error. Strokes in the pupil exceeded 1 um at a couple of points. Stroke outside the pupil, in the "guard band" actuators, was larger than this. It is not likely that a cryogenic DM can achieve these strokes at a 3.75 mm pitch. A larger pupil, fewer DM actuators, or other mitigation will be required.

was larger than this. It is not likely that a cryogenic DM can achieve these strokes at a 3.75 mm pitch. A larger pupil, fewer DM actuators, or other mitigation will be required.

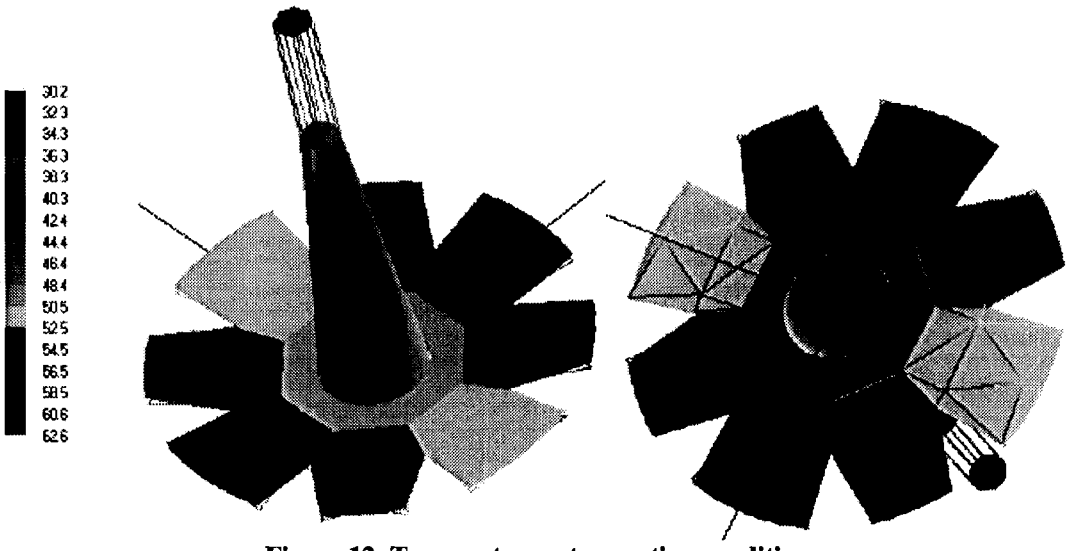

Figure 12. Temperatures at operating conditions.

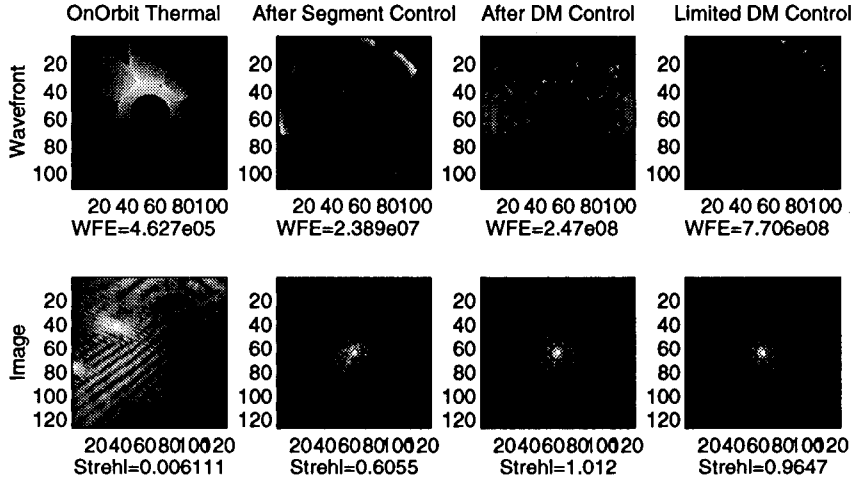

Figure 13. Ground-to-orbit thermal response, pre- and post-control.

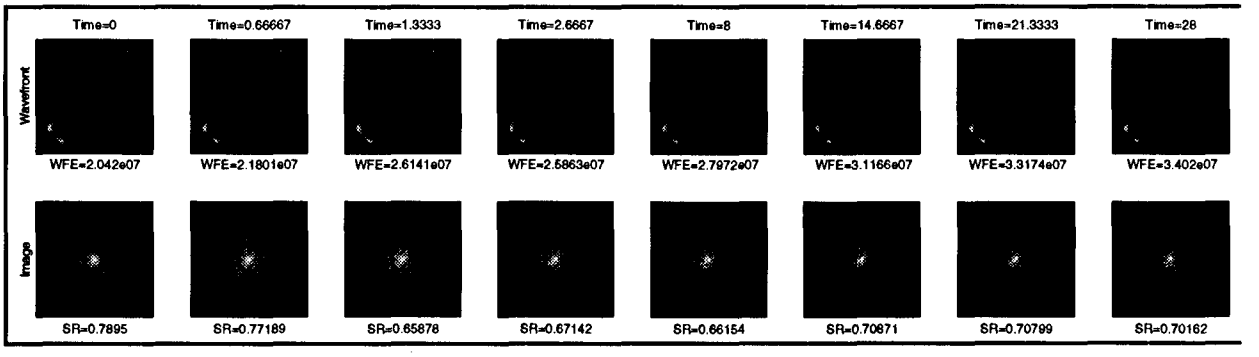

Figure 13. Transient thermal response, worst-case slew.

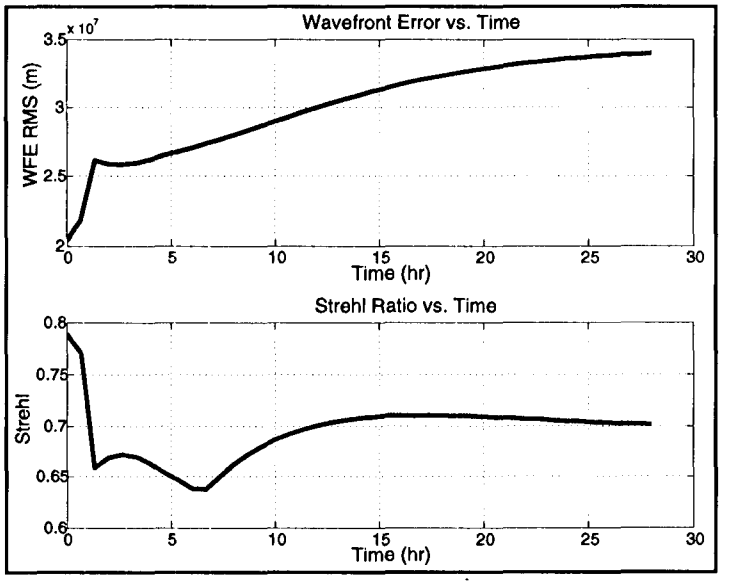

Figure 14. Transient thermal response summary, worst-case slew.

8.CONCLUSION

The baseline NGST optical control system described here is broadly capable, and offers a simple starting point for further refinement as the NGST design firms up.

In designing this system, we have tried to adopt the simplest approach that has a chance of working whenever we have had a choice. At a few points we know about, and perhaps at others we don't yet know about, these choices may have to be revised. The use of a DM, rather than segment deforming actuators, yields a mechanically less complex system -- but can a cryogenic DM be built with adequate performance and good reliability? Relying on passive structural stability to hold alignments during observations eliminates the need for segment metrology -- but can the material CTEs be tailored well enough to make this approach work?

These are the questions that need to be answered as NGST moves towards project status. With the NGST integrated modeling, we have begun to put into place a framework in which to address these questions.

9.ACKNOWLEDGEMENT

This work was performed at the Jet Propulsion Laboratory, California Institute of Technology, under contract with NASA.

10.REFERENCES

1. B. D. Seery, "Next generation space telescope (NGST)," SPIE Symposium on Astronomical Telescopes and Instrumentation, Paper 3356-01, Kona HI (1998).
2. J. C. Mather, E. P. Smith, H. S. Stockman, "Scientific metrics for the next generation space telescope," SPIE Symposium on Astronomical Telescopes and Instrumentation, Paper 3356-02, Kona HI (1998).
3. A.E. Bryson and Y.C. Ho, *Applied Optimal Control*, Halsted Press, 1969.
4. J. C. Mather, E. P. Smith, H. S. Stockman, "Scientific metrics for the next generation space telescope," SPIE Symposium on Astronomical Telescopes and Instrumentation, Paper 3356-02, Kona HI (1998).
5. G. E. Mosier, M. Femiano, K. Ha, P. Y. Bely, R. Burg, D. C. Redding, A. Kissil, J. Rakoczy, L. Craig, "Integrated modeling environment for systems-level performance analysis of the next generation space telescope," SPIE Symposium on Astronomical Telescopes and Instrumentation, Paper 3356-08, Kona HI (1998).